Biochimica et Biophysica Acta 1838 (2014) 2985–2993

Contents lists available at ScienceDirect

Biochimica et Biophysica Acta

journal homepage: www.elsevier.com/locate/bbamem

Relationship between peptide structure and antimicrobial activity as studied by *de novo* designed peptides

Jianbo Sun [a,1], Yuqiong Xia [b,1], Dong Li [c], Quan Du [c,*], Dehai Liang [a,**]

[a] Beijing National Laboratory for Molecular Sciences and the Key Laboratory of Polymer Chemistry and Physics of Ministry of Education, College of Chemistry and Molecular Engineering, Peking University, 100871 China
[b] School of Life Sciences and Technology, Xidian University, Xi'an, Shaanxi 710126, China
[c] State Key Laboratory of Natural and Biomimetic Drugs, School of Pharmaceutical Sciences, Peking University, Beijing 100871, China

ARTICLE INFO

Article history:
Received 19 April 2014
Received in revised form 5 July 2014
Accepted 15 August 2014
Available online 23 August 2014

Keywords:
Antimicrobial peptide
Membrane leakage
Fusion
Aggregation

ABSTRACT

As fundamental components in innate immunity, antimicrobial peptides (AMPs) hold great potentials in the treatment of persistent infections involving slow-growing or dormant bacteria in which, selective inhibition of prokaryotic bacteria in the context of eukaryotic cells is not only an essential requirement, but also a critical challenge in the development of antimicrobial peptides. To identify the sequence and structural properties critical for antimicrobial activity, a series of peptides varying in sequence, length, hydrophobicity/charge ratio, and secondary structure, were designed and synthesized. Their antimicrobial activities were then tested using *Escherichia coli* and HEK293 cells, together with several index activities against model membrane, including liposome leakage, fusion, and aggregation. While no evident correlation between the antimicrobial activity and the property of the peptides was observed, common activities against model membrane were nevertheless identified for the active antimicrobial peptides: mediating efficient membrane leakage, negligible membrane fusion and liposome aggregation. Therefore, in addition to identifying one highly active antimicrobial peptide, our study further sheds light on the design principle for these molecules.

1. Introduction

Antimicrobial peptides are abundant and diverse group of molecules produced and distributed in a variety of invertebrate, plant, and animals species, serving as "defender" against bacteria, fungi, viruses, and other invasion conceivable substances [1]. Although their antibacterial activity was proposed to derive mainly from their membrane disruption capability, recent studies suggested that AMPs also inhibited the formation of cell walls, as well as the synthesis of DNA, RNA and proteins [2].

AMPs are peptides with a length less than 100 amino acids. Their amino acid composition, amphiphilicity, cationic charge, and size allow them to attach to and insert into the bilayer membrane of bacteria, as well as to achieve selectivity between prokaryotic bacteria and eukaryotic mammalian cells. To elucidate the relationship between peptide structures and antibacterial activities, a variety of peptides differing in size, hydrophobicity, charge density, as well as secondary structure were studied [3–11]. Generally, higher hydrophobicity of AMPs led to enhanced membrane disturbance and compromised cellular selectivity [12], while higher charge density led to enhanced electrostatic interaction between peptides and membrane, and lowered toxicity to mammal cells [6,13]. In addition, secondary structure of AMPs also showed significant influence. Studies indicated that AMPs stayed random in water, and formed α-helix upon interacting with membrane [7]. In response to the environment stimulations, change of the peptide secondary structure can cause more efficient membrane leakage [14]. The effect was more evident for less-charged membrane [9]. It was also found that AMPs with increasing length were more destructive to membranes [15]. Even though the effect of individual peptide property has been well understood, combinational effects of multiple properties are rarely investigated, which presents a critical challenge for the development of high performance AMPs [11].

Technically, the performances of AMPs are usually characterized by liposome leakage, using large unilamellar vesicles (LUVs) or giant unilamellar vesicles (GUV) as the model membrane. The degree of leakage is taken as a criterion to evaluate the membrane destroying capability of the AMPs [5,10,16]. The kinetics of the liposome leakage are also used to measure the interactions between AMPs and membranes [17]. Despite these investigations, the liposome leakage is not directly related to the antibacterial activity of AMPs. Particularly for LUVs, the leakages are often found to be accompanied with liposome aggregation and membrane fusion [18]. However, the underlying mechanisms and their effects on the antibacterial activity of AMPs have not been defined.

* Corresponding author. Tel./Fax: +86 10 82805780.
** Corresponding author. Tel./Fax: +86 10 62756170.
E-mail addresses: quan.du@pku.edu.cn (Q. Du), dliang@pku.edu.cn (D. Liang).
[1] These authors contributed equally to this work.

http://dx.doi.org/10.1016/j.bbamem.2014.08.018
0005-2736/

Herein, we designed and tested a series of peptides, which varied in terms of peptide sequence, length, hydrophobicity/charge ratio, and secondary structure (Table 1). To make the results comparable, only two types of amino acids, lysine and leucine mainly, were used for each peptide, with an exception of K_{14} consisting of only lysine. The peptides were designed to be with a sequence of bola-typed ($K_3L_8K_3$) or surfactant-like (K_6L_8). Peptides with the sequence of $(KL_2KL_2K)_2$ or $(KL_2KL_3)_2$ were designed to take an amphiphilic α-helical structure, according to the helical wheel diagram prediction. To evaluate the influence of the hydrophobicity and secondary structure, the leucine in $K_3L_8K_3$ was replaced by either isoleucine or valine, in peptide $K_3I_8K_3$ and $K_3V_8K_3$. To evaluate the influence of peptide length, repeated sequence was designed for peptide $K_6L_{16}K_6$, compared to peptide $K_3L_8K_3$. Using LUVs composed of 1,2-dipalmitoyl-*sn*-glycero-3- phosphocholine (DPPC) and 1,2-dipalmitoyl -*sn* -glycero-3-phospho-(1′-*rac*-glycerol) (DPPG), the kinetics of membrane leakage, liposome aggregation, and membrane fusion was comparatively investigated. Antibacterial activity of the peptides was investigated with *E. coli*, while their cytotoxicity was examined with HEK293 cells.

2. Materials and methods

2.1. Materials

1,2-dipalmitoyl-*sn*-glycero-3-phosphocholine (DPPC, >99%), $TbCl_3 \cdot 6H_2O$, and 2,6-Pyridinedicarboxylic acid (DPA) were purchased from Sigma. Chloroform solution of 1,2-dipalmitoyl-*sn*-glycero-3-phosphoethanolamine-N-(7-nitro-2-1,3-benzoxadiazol-4-yl) (NBD-DPPE, ammonium salt), 1,2-dipalmitoyl-*sn*-glycero-3-phosphoethanolamine-N-(lissamine rhodamine B sulfonyl) (Rh-DPPE, ammonium salt), and 1,2-dipalmitoyl-*sn*-glycero-3-phospho-(1′-*rac*-glycerol) (DPPG, sodium salt) were purchased from Avanti Polar Lipids, Inc. All peptides (purity >98%) were synthesized by GL Biochem (Shanghai, China) Ltd. Mueller–Hinton Broth was from Hope-Bio Technology co. Ltd. Fetal bovine serum was from HyClone Laboratories. Inc. Penicillin and streptomycin were from Life Technologies, Gibco. Milli-Q water (18.2 MΩ.cm) was used in all the experiments.

2.2. Circular dichroism spectra

Peptides were individually dissolved in Milli-Q water and sonicated for 5–10 s to obtain stock solution with a concentration of 1.00 or 0.25 mg/mL. Milli-Q water or trifluoroethanol (TFE) was used to dilute the stock solution. The circular dichroism (CD) spectra were measured from 190 to 250 nm at 50 °C using a JASCO J-810 spectrometer (AVIV, USA), with a 1.0 cm path length cuvette. Temperature was controlled by using a PolyScience programmable temperature controller. Peptides in Milli-Q water (25 μM) or 50% TFE (12.5 μM) was used in the measurement. For each peptide, three independent assays were performed.

Table 1
The sequences and secondary structures of peptides in 50% TFE.

Name	Sequence	α-helix	β-sheet	β-turn	random
$(KL_2KL_3)_2$	Ac-KLLKLLLKLLKLLL-amide	0.58	0.03	0.11	0.27
$(KL_2KL_2K)_2$	Ac-KLLKLLKKLLKLLK-amide	0.58	0.04	0.12	0.27
$K_3L_8K_3$	Ac-KKKLLLLLLLLKKK-amide	0.62	0.06	0.12	0.22
K_6L_8	Ac-KKKKKKLLLLLLLL-amide	0.50	0.06	0.15	0.28
$K_3I_8K_3$	Ac-KKKIIIIIIIIKKK-amide	0.35	0.17	0.20	0.30
$K_3V_8K_3$	Ac-KKKVVVVVVVVKKK-amide	0.10	0.34	0.18	0.26
$K_6L_{16}K_6$	Ac-KKKKKLLLLLLLL-LLLLLLLLKKKKKK-amide	0.41	0.12	0.18	0.29
K_{14}	Ac-KKKKKKKKKKKKKK-amide	N/A	N/A	N/A	N/A

2.3. Preparation of LUVs

DPPC/DPPG LUVs were prepared using the Bangham method [19]. In brief, DPPC solution (chloroform) and DPPG solution (methanol, v/v = 9/1) were added into a 50 mL pyriform flask at a molar ratio of 1:1, and mixed with Teflon beads. The organic solvent was removed at 50 °C under reduced pressure, followed by vacuuming overnight. The liposome film was then hydrated with Hepes buffer (pH 7.40, 20 mM Hepes, 150 mM NaCl, 0.1 mM EDTA) at 50 °C on a rotary evaporator for 1 h, with occasional vortexing. Using a mini-extruder (Avanti Polar Lipids, Inc.) and a polycarbonate filter with 100 nm pore size, liposome solution was extruded at 50 °C for 21 times. DPPC/DPPG liposome labeled with fluorescent probes (Rh-DPPE) was prepared similarly. The final concentration of liposome was determined by a modified Bartlett method [20]. The stock solution of liposome was then diluted to 15.6 μM in Hepes buffer.

2.4. Liposome leakage assay

Liposome leakage assays were performed at 50 °C using fluorescence $TbCl_3$-DPA [21]. Tb/DPA-loaded liposome (10 mg/mL) was prepared in a buffer (1.25 mM $TbCl_3$, 25 mM Na-citrate, 25 mM DPA, 60 mM NaCl, 20 mM Na-Hepes, pH 7.4). The non-encapsulated reagents were removed by filtrating the solution through a Sephadex G-25 M column (column size, 1.0 × 20 cm; elution buffer: 150 mM NaCl, 1 mM EDTA, 20 mM Na-Hepes, pH 7.4). The fluorescence intensity of the Tb/DPA-loaded liposome was set as I_∞. 100% leakage was obtained by adding 0.05 wt.% Triton X-100 to the "Tb/DPA-loaded" liposome (total lipid concentration 15.6 μM). The fluorescence intensity at 100% leakage was set as I_0. Liposome leakage in the presence of peptide was measured with a Fluoromax-4 spectrophotofluorimeter. The excitation and emission wavelengths were 280 and 543 nm, respectively. A cutoff filter at 430 nm was placed in the emission path to eliminate the contributions from the scattered light. In accordance with the molar ratio of 0.053 after adding the peptides, the fluorescence intensity of the mixture was denoted as I_t, and the percentage of liposome leakage was calculated according to the equation:

$$\text{Leakage}(\%) = 100 \times (I_\infty - I_t)/(I_\infty - I_0) \quad (1)$$

2.5. Laser light scattering

A commercialized spectrometer equipped with a BI-TurboCo Digital Correlator (BI-200SM, Brookhaven Instruments Corporation, Holtsville) was used to perform both static light scattering (SLS) and dynamic light scattering (DLS), over a scattering angular range of 20–120°. A vertically polarized, 100 mW solid-state laser (GXC-III, CNI, Changchun, China) operating at 532 nm was used as the light source.

In DLS, the intensity–intensity time correlation function $G^{(2)}(\tau)$ in the self-beating mode was obtained on the basis of

$$G^{(2)}(\tau) = A\left[1 + \beta\left|g^{(1)}(\tau)\right|^2\right] \quad (2)$$

where A is the measurement base line, β is a coherence factor, τ is the delay time, and $g^{(1)}(\tau)$ is the normalized first-order electric field time correlation function. $g^{(1)}(\tau)$ was related with the line width distribution $G(\Gamma)$ by

$$g^{(1)}(\tau) = \int_0^\infty G(\Gamma) e^{-\Gamma\tau} d\Gamma \quad (3)$$

By using a Laplace inversion program, CONTIN [22], the normalized distribution function of the characteristic line width $G(\Gamma)$ was obtained.

The average line width $\overline{\Gamma}$ was calculated according to $\overline{\Gamma} = \int \Gamma G(\Gamma) d\Gamma$. $\overline{\Gamma}$ was a function of both C and q, which was expressed as

$$\overline{\Gamma}/q^2 = D(1 + k_d C)\left[1 + f\left(R_g q\right)^2\right] \quad (4)$$

where k_d, and f are the diffusion second virial coefficient and a dimensionless constant, respectively.

D was further converted into the hydrodynamic radius R_h by using the Stokes–Einstein equation

$$D = k_B T/6\pi\eta R_h \quad (5)$$

where k_B, T and η are the Boltzmann constant, the absolute temperature and the viscosity of the solvent, respectively.

For aggregation assays, peptide aqueous solutions of 25 μM were added into 7.8 μM/7.8 μM DPPC/DPPG liposomes at 50 °C. After vortexing for 30 s at 1200 rpm, the solutions were measured by laser light scattering. The molar ratio of peptides/liposomes was defined as $\rho_{p/l}$.

2.6. Membrane fusion assay

Membrane fusion of liposomes was determined by the fluorescence resonant energy transfer between NBD-DPPE and Rh-DPPE [23]. NBD-DPPE and Rh-DPPE were incorporated into one population of liposomes ("labeled liposomes") at 1 mol% each, a probe concentration at which there was significant NBD quenching by Rh. The labeled vesicles were then mixed with vesicles containing no fluorescent phospholipids ("unlabeled liposomes") at a ratio of 1:9. The residual fluorescence intensity I_0 was taken as 0% of the maximum fluorescence. The total lipid concentration was 15.6 μM. The peptide was then added. The measured fluorescence was denoted as I_t. Complete intermixing of all the bilayers upon fusion would be expected to result in a membrane containing 0.1 mol% each of the two fluorescent phospholipids. The liposome containing 0.1 mol% of each probes, but prepared separately, was used to calibrate the 100% maximum fluorescence intensity I_∞. The percentage of fusion was calculated as $F(\%) = 100 \times (I_t - I_0)/(I_\infty - I_0)$.

2.7. Antimicrobial assay

Antimicrobial assays were performed with *E.* coli (ATCC25922), using Broth Microdilution protocol established by the Clinical and Laboratory Standards Institute (CLSI) [24]. Stock solution of each peptide was serially diluted at a 1/2 ratio.

E. coli was cultured for 4 h in Mueller–Hinton Broth (MHB). It was first adjusted to 0.5 McFarland standard in fresh broth medium, and then diluted at 1:200. 100 μL bacteria solution and 100 μL peptide solution in MHB were mixed, added into each well of a 96-well plate in triplicate. Bacteria- and peptide-free MHB was used as a control. After an incubation of 24 h at 37 °C, the growth of the bacteria was recorded visually. The minimum inhibitory concentration (MIC) was determined as the lowest concentration at which no growth occurred. Each measurement was repeated for 3 times, and the average was calculated.

2.8. Cytotoxicity assay

HEK293 cells were grown in Dulbecco's modified Eagle's medium supplemented with 10% fetal bovine serum (HyClone Laboratories, Inc.), 100 units/mL penicillin, and 100 μg/mL streptomycin (Life Technologies, Gibco).

To evaluate the cytotoxicity of the peptides, HEK293 cells were seeded in 96-well plates at ~6×10^3 cells/well one day before transfection. After allowing them to grow overnight, the cells were treated with peptides at concentrations of 64, 32, 16 and 8 μg/mL, and further incubated for 24 h. Then, the culture medium was removed and 20 μL of CCK-8 reagent (Dojindo Molecor Technologies, Inc.) was added into each well, and incubated for 2 h under normal condition. At the end of incubation, the absorbance was read at 450 nm with a reference wavelength of 650 nm. The absolute absorbance (OD_{net450}) is OD_{450} minus OD_{650}. For comparison of relative viability, all data were presented as the mean percentage ± SEM in pentaplicate samples compared to the absorbance value of the mock-treated cells. Cell viability was calculated as:

$$\text{Cell viability } (\%) = \left(OD_{net450(sample)}/OD_{net450(mock)}\right) \times 100\% \quad (6)$$

where $OD_{net450(sample)}$ is the absorbance of the transfected cells at 450 nm and $OD_{net450(control)}$ is the absorbance of the mock control (non-transfected cells) at 450 nm.

3. Results

3.1. Secondary structures of candidate AMPs

CD measurements were performed to examine the second structures of the designed AMP peptides, in aqueous and in hydrophobic solutions. In the study, pure water instead of Hepes buffer, was used as solvent to remove noise signal of NaCl. For the same reason, 50% TFE solution was used to mimic the hydrophobic environment of the membrane [25]. CD spectra of the peptides in water or 50% TFE were obtained and shown in Fig. 1. The results indicated that, while peptide $(KL_2KL_3)_2$ and $K_6L_{16}K_6$ were mainly in an α-helix structure in water, all the other peptides took a random structure. In 50% TFE solution, all the peptides took an ordered secondary structure, with an exception of K_{14} existing still in a random structure.

To quantitatively analyze the structures of the peptides (except K_{14}) in hydrophobic solution, CDpro software (SELCON3 method) [26] was used to calculate the content of various secondary structures. As shown in Table 1, all the 14-mer peptides composing of K and L ($(KL_2KL_3)_2$, $(KL_2KL_2K)_2$, $K_3L_8K_3$ and K_6L_8) formed high content (> = 50%) α-helix in a hydrophobic environment. Compared with other peptides, the α-helix content was relatively low for $K_3I_8K_3$ (35%) and in $K_6L_{16}K_6$ (41%). In contrast, $K_3V_8K_3$ peptide formed mainly β-sheet structure (34%), with α-helix content of only 10%.

To reveal the structural details of the α-helixes formed in hydrophobic solution, their helical wheel diagrams were drawn. As shown in Fig. 2, the α-helix formed by $(KL_2KL_3)_2$ or $(KL_2KL_2K)_2$ was amphiphilic across the diameter, where the charged residues were located on one side and the hydrophobic residues were located on the opposite side. The two structures differed in the ratios of the charged residues, 1/3 in $(KL_2KL_3)_2$ and 1/2 in $(KL_2KL_2K)_2$. The amphiphilic feature was presented for the other peptides, the charged residues, however, distributed along the axis of the helix, instead of across the diameter. As shown in Fig. 2, a hydrophobic block located at one side of the α-helix formed by K_6L_8; whereas for $K_3L_8K_3$, a hydrophobic block formed in the middle of the structure. The α-helixes formed by $K_3I_8K_3$ and $K_6L_{16}K_6$ were similar to that of $K_3L_8K_3$.

3.2. Effects on liposome leakage

To mimic the interaction between AMPs and the negatively charged bacterial membrane, an anionic liposome composing of DPPC and DPPG at 1/1 molar ratio was chosen as the model membrane. Even though it is different from the bacterial membrane, the basic principles should apply when studying the physical interactions between peptides and lipids. DPPC and DPPG were completely miscible at temperatures below or above the melting point, no phase separation occurred. The charge content was fixed at 50% to facilitate the electrostatic interaction between liposome and peptide.

Liposome leakage assay was often used to evaluate the membrane disruption capacity of AMPs. In our study, the leakage of liposome was

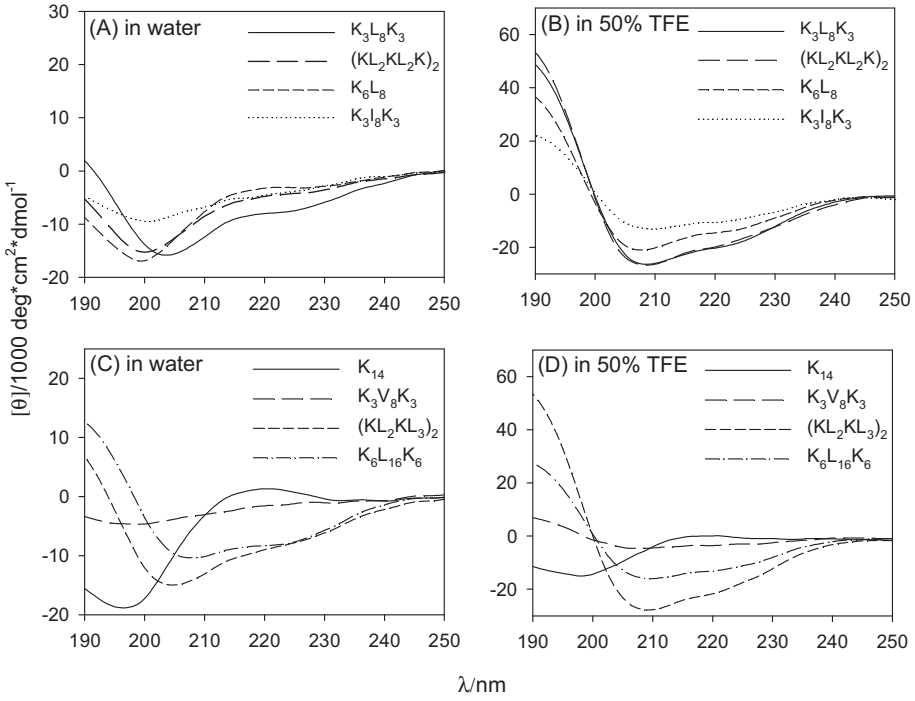

Fig. 1. CD spectra of peptides at a concentration of 25 μM in water (A and C), and at a concentration of 12.5 μM in 50% TFE (B and D).

monitored by tracing the remaining $Tb(DPA)_3$ fluorescence, after mixing the liposome with a given peptide. Fig. 3 compares the leakage curves of the liposome in the presence of the studied peptides. The leakage in Fig. 3A is slightly above 100%, which is within the experimental error. As shown in Fig. 3, all the peptides caused evident liposome leakage at 50 °C. The leakage curves of all the bola-typed peptides, including $K_3L_8K_3$, $K_3I_8K_3$, $K_3V_8K_3$, and $K_6L_{18}K_6$ can be fitted by a double exponential growth model (Eq. 8), while the rest showed a simple exponential rise to maximum and can be fitted by Eq. 7. The characteristic time(s) of leakage calculated by Eqs. 7 and 8, and the leakage percentage in 1 h, are listed in Table 2.

$$y = y0 + A\left(1 - \exp\left(-\frac{t}{\tau_0}\right)\right) \tag{7}$$

$$y = y0 + A\left(1 - \exp\left(-\frac{t}{\tau_0}\right)\right) + B\left(1 - \exp\left(-\frac{t}{\tau_1}\right)\right) \tag{8}$$

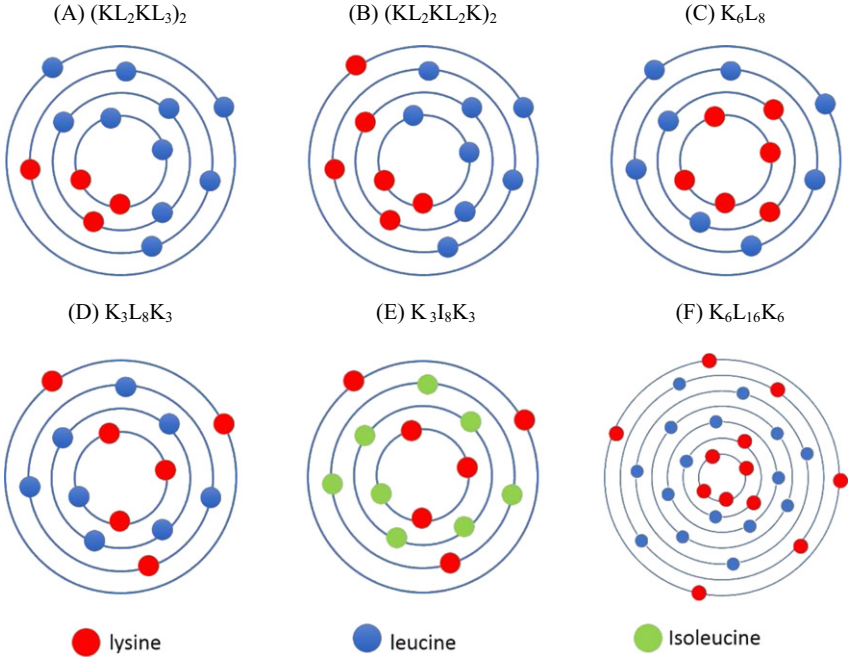

Fig. 2. Helical wheel diagrams of amphiphilic α-helical peptides $(KL_2KL_3)_2$ (A) and $(KL_2KL_2K)_2$ (B), surfactant-like peptide K_6L_8 (C), bola-typed peptide $K_3L_8K_3$ (D), $K_3I_8K_3$ (E), and $K_6L_{16}K_6$ (F).

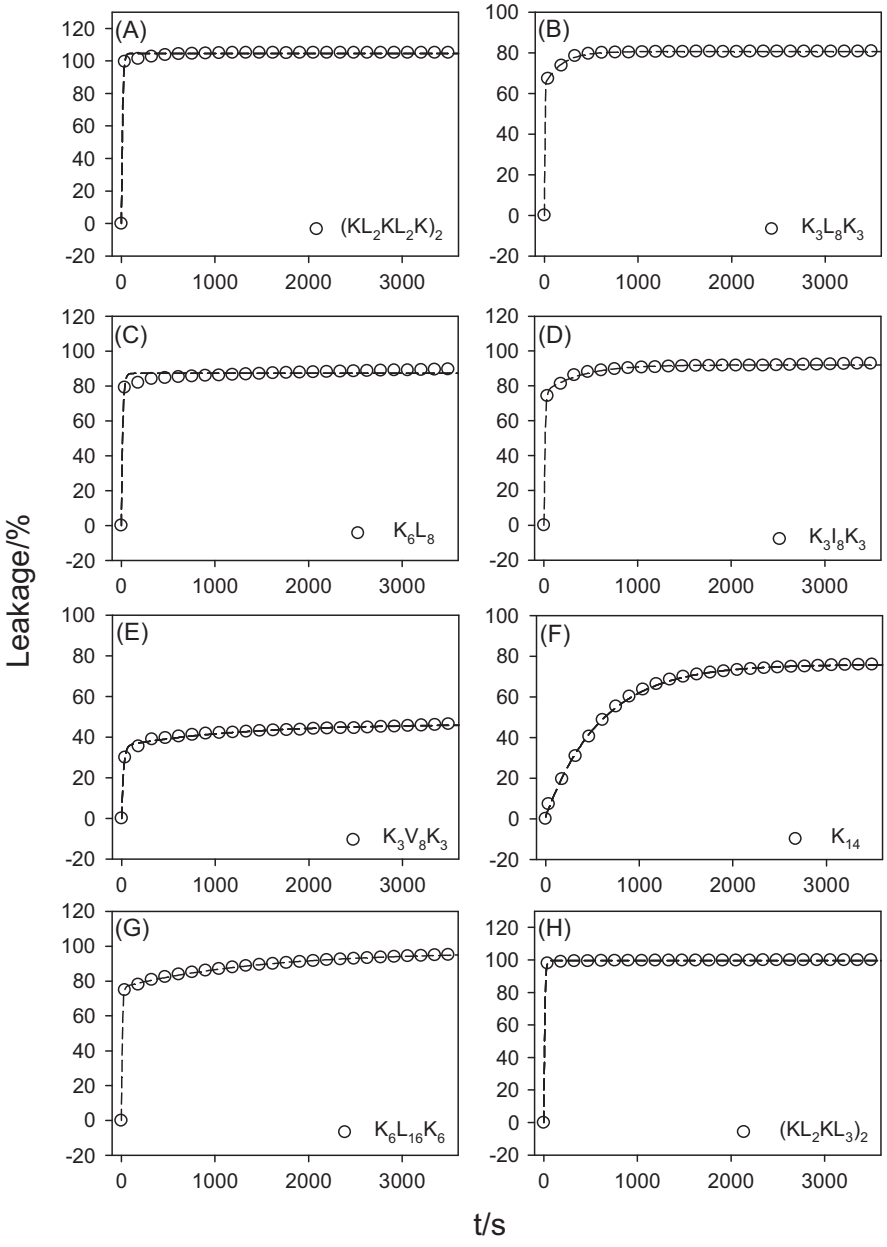

Fig. 3. Liposome leakage mediated by peptides: (A) $(KL_2KL_2K)_2$, (B)$K_3L_8K_3$, (C) K_6L_8, (D) $K_3I_8K_3$, (E) $K_3V_8K_3$, (F) K_{14}, (G) $K_6L_{16}K_6$, and (H) $(KL_2KL_3)_2$. The concentration of the peptide is 25 μM; C(DPPC/DPPG) = 15.6 μM; $\rho_{p/l} = 0.053$. The dashed curves are the fitting of the data. The data in Panels A, C, F, and H are fitted by $y = y0 + A\left(1-\exp\left(-\frac{t}{\tau_0}\right)\right)$, while the rest are fitted by $y = y0 + A\left(1-\exp\left(-\frac{t}{\tau_0}\right)\right) + B\left(1-\exp\left(-\frac{t}{\tau_1}\right)\right)$.

Table 2
Experimental data with model cell and MIC.[a]

	MIC/μM	Survive fraction in MIC/%	Leakage kinetics[b]	Aggregation kinetics[c]	Fusion kinetics[b]
$(KL_2KL_2K)_2$	2	122 ± 12	100(12 s)	2.0(N/A)	10(N/A)
$K_3L_8K_3$	9	108 ± 1	80(1.1 s/185 s)*	16(670 s)	80(380 s)
K_{14}	9	102 ± 5	70(600 s)	20(25 s)	67(1200 s)
$K_3V_8K_3$	10	97 ± 2	40(20 s/1200 s)*	11(360 s)	40(300 s)
K_6L_8	18	116 ± 3	83(15 s)	20(40 s)	80(0.4 s/1000 s)*
$(KL_2KL_3)_2$	19	13 ± 5	100(10 s)	7.0(63 s)	60(10 s)
$K_3I_8K_3$	N/A	N/A	93(12 s/400 s)*	16(140 s)	80(10 s/770 s)*
$K_6L_{16}K_6$	N/A	N/A	95(10 s/1400 s)*	Precipitate	Precipitate

*The characteristic times are calculated by fitting the curves through $y = y0 + A\left(1-\exp\left(-\frac{t}{\tau_0}\right)\right) + B\left(1-\exp\left(-\frac{t}{\tau_1}\right)\right)$;the others are calculated by fitting the curves through $y = y0 + A\left(1-\exp\left(-\frac{t}{\tau_0}\right)\right)$.

[a] Minimal inhibitory concentration is defined as the point of nearly 100% inhibition of *E. coli*'s growth compared with the control.
[b] Fusion or leakage percentage in 1 h. The numbers in the brackets show the corresponding characteristic time.
[c] Final aggregation number. The characteristic aggregation time is shown in the brackets.

The leakage was very fast in some cases. Since the initial value was known, the fitting still yielded valid kinetic data for comparison. As shown in Table 2, all the 14-mer peptides containing both K and L resulted in faster leakage rates and higher leakage content in 1 h. Replacing L by I or V compromised the leakage by either decreasing the kinetics ($K_3I_8K_3$) or lowering the leakage percentage ($K_3V_8K_3$). In the case of $K_3V_8K_3$, the leakage content in 1 h was only 40%, much lower than those of the others. K_{14} contains no hydrophobic residues. Its leakage rate was the slowest among the tested peptides. The leakage of the liposome in the presence of the bola-typed peptides can be described by a function of double exponential growth (Eq. 8), and the rate at each stage followed the order of $K_3L_8K_3 < K_3I_8K_3 < K_3V_8K_3$, suggesting that the bola-typed peptides disrupted the membrane in two steps, and the degree of hydrophobicity was important at each step. Taken together, these data indicated that the hydrophobic residues played a key role in disrupting the membrane.

3.3. Antimicrobial activity

Antibacterial activity of the peptides were tested with *E. coli*. A MIC value was determined for each peptide, using Broth microdilution protocol [19,27]. Melittin, a natural antimicrobial peptide, was included in the assays as a reference. While no antibacterial activity was observed for $K_3I_8K_3$ and $K_6L_{16}K_6$ at concentrations of 1.0–64 μg/mL, the activity of the other six peptides were presented in Fig. 4. From which, a MIC value was obtained for each peptide and summarized in Table 2. According to the MICs, the peptides were divided into three groups. Group 1 contains $(KL_2KL_2K)_2$ only, whose MIC value (2 μM or 8 μg/mL) is the lowest among the tested peptides including melittin (3 μM) (Fig. S1). Group 2 contains K_{14}, $K_3V_8K_3$, $K_3L_8K_3$, K_6L_8, and $(KL_2KL_3)_2$, whose MIC values range from 9 to 18 μM (16–32 μg/mL). Group 3 contains $K_3I_8K_3$ and $K_6L_{16}K_6$. Interestingly, no antibacterial activity was observed for this group (Fig. S1).

To evaluate their cytotoxicities, CCK-8 assays were performed with cultured HEK293 cells, at concentrations around the identified MIC. The results were presented in Block 2 of each panel in Fig. 4, and summarized in Table 2. It was found that, with the exception of $(KL_2KL_3)_2$, all the peptides were safe to normal cells at the MIC doses.

The data in Table 2 revealed a non-proportional correlation between liposome leakage and antibacterial activity. For example, around MIC concentration, $K_3I_8K_3$ caused an extensive liposome leakage, however, no antibacterial activity was observed. Both K_{14} and $K_3V_8K_3$ were weak in membrane disrupting as demonstrated by the long leakage characteristic time or low leakage content within 1 h. However, their MIC values were relatively low.

3.4. Effects on liposome aggregation and membrane fusion

To further characterize the behavior of the peptides, two other index assays, liposome aggregation and membrane fusion, were carried out.

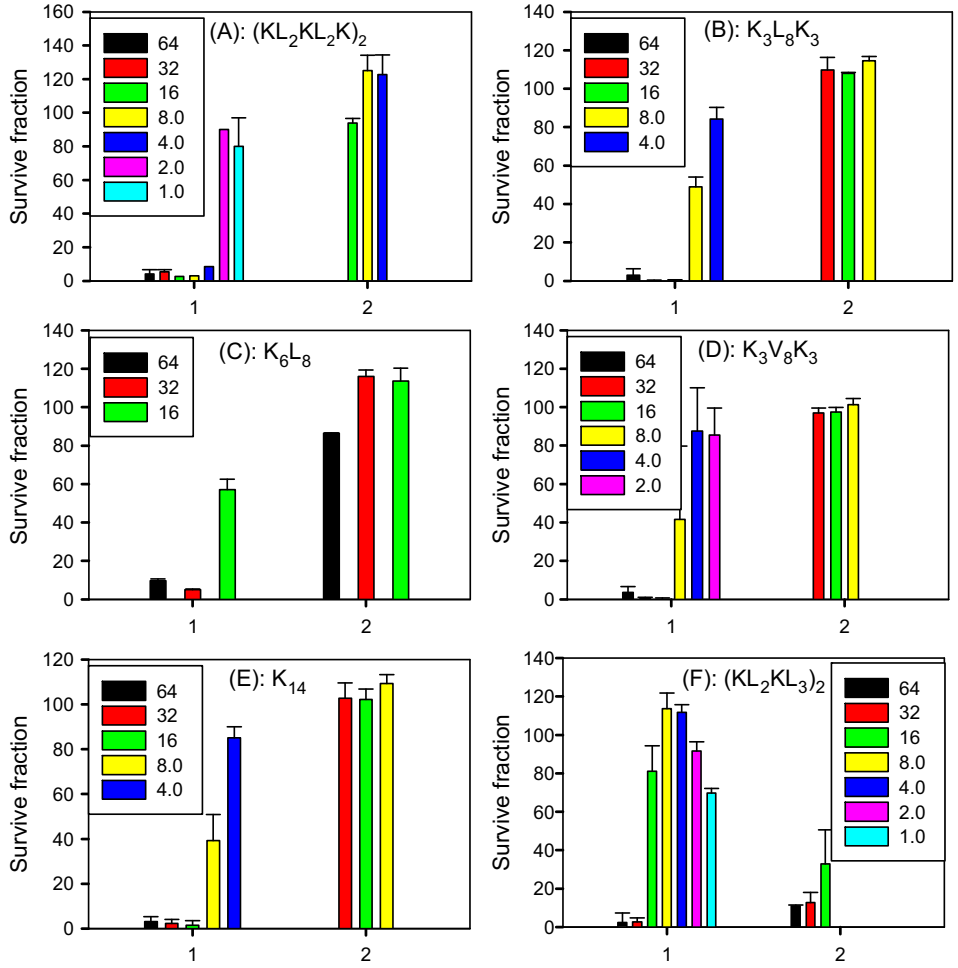

Fig. 4. Antimicrobial activities of candidate AMPs: (A) $(KL_2KL_2K)_2$, (B)$K_3L_8K_3$, (C) K_6L_8, (D) $K_3V_8K_3$, (E) K_{14}, and (F) $(KL_2KL_3)_2$ (all peptide concentrations are mass concentration in ug/mL). Blocks 1 and 2 in each panel show the activities on *E. coli* and HEK293 cells, respectively.

Liposome aggregation and membrane fusion accompanied membrane leakage in most cases, occurring earlier or at the same time [18,28]. The kinetics of liposome aggregation and membrane fusion was monitored using time-resolved laser light scattering (LLS) and FRET. The experiment settings were the same as those of liposome leakage assay. The results showed that all the peptides caused liposome aggregation with varying kinetics. The degree of the aggregations was also different, as quantitatively measured by the aggregation number. Since the scattered intensity I is proportional to the molecular weight M at fixed concentration [29], the aggregation number M/M_0 can be estimated using I/I_0, with I_0 and I being the excess scattered intensity of the liposome before and after the addition of peptide.

Fig. 5A compares the LLS data of $(KL_2KL_2K)_2$, K_6L_8, and $K_3L_8K_3$. LLS data of the other peptides were shown in Fig. S2. Except for $(KL_2KL_2K)_2$ and $K_6L_{18}K_6$, Similar aggregation curves were observed for the other peptides. An overshoot curve was observed for $(KL_2KL_2K)_2$ at the very beginning of the assays; while for $K_6L_{18}K_6$, extensive precipitation occurred in the assays. Monomodal distributions were observed during the aggregation process (Fig. 5C). The aggregate size and the distribution varied over the course, depending on the type of the peptides (Fig. 5B). Fitting the aggregation curves by Eq. 7 or Eq. 8 yielded a characteristic time for most of the peptides. These values, together with the aggregation numbers after reaching equilibrium, are shown in Table 2. The lowest aggregation number was found with $(KL_2KL_2K)_2$, followed by $(KL_2KL_3)_2$, and $K_3V_8K_3$. The other peptides resulted in heavy aggregation of the liposomes, even led to macrophase separation in the case of $K_6L_{18}K_6$.

Using a similar approach, the kinetics of membrane fusion was determined for each peptide. Fig. 5D compares the membrane fusion mediated by $(KL_2KL_2K)_2$, K_6L_8, and $K_3L_8K_3$. Similar fusion curves were observed for the other peptides except $K_6L_{16}K_6$, which led to a heavy precipitation (Fig. S3). The characteristic time and the fusion percentage in 1 h are listed in Table 2. The fastest fusion occurred in the presence of $(KL_2KL_3)_2$, K_6L_8, and $K_3I_8K_3$, while K_{14} showed the slowest fusion process probably owing to the lack of hydrophobic residues. The degree of fusion was the lowest for $(KL_2KL_2K)_2$, only about 10%. $K_3V_8K_3$ also led to low level (40%) of membrane fusion.

4. Discussion

A comprehensive data set including the antibacterial activity, the kinetics of membrane leakage, aggregation and fusion, was presented in Table 2. Correlation analysis found that neither the liposome leakage nor the content of α-helix structure could serve as a sole criterion to predict the antimicrobial activity of the peptides. For example, neither K_{14} nor $K_3V_8K_3$ formed prominent α-helix conformation in hydrophobic environment, they however exhibited moderate antimicrobial activities. In the cases of $K_3I_8K_3$ and $K_6L_{16}K_6$, a nearly 100% liposome leakages were mediated in 1 h; however, no antimicrobial activity was identified.

Among the tested peptides, $(KL_2KL_2K)_2$ showed the best performance. Its MIC value was 2 μM, a value comparable to that of melittin [30], and much lower than the other peptides. The major difference between $(KL_2KL_2K)_2$ and the other peptides was that it induced negligible liposome aggregation and membrane fusion while mediating heavy membrane leakage. From a view of physics, liposome aggregation, fusion, and leakage followed distinct mechanisms. The aggregation was driven mainly by inter-particle attraction, for example electrostatic interaction. It was a strong and long-ranged interaction, effective in pulling the oppositely charged particles together. This was demonstrated by the fast and efficient aggregation in the presence of K_{14}. The fusion of membrane depends not only on the inter-particle attraction force, but also on the merging of the outer leaflet of the membrane, which involves hydrophobic interactions. Therefore, liposome aggregation was a prerequisite for fusion. As shown in Table 2, obvious fusion could not occur without aggregation. In contrast, liposome leakage, which resulted from the disruption of the membrane, was closely related to the antimicrobial activity. The pore-forming mechanism, where the interaction mainly was located inside the membrane, was believed to be the

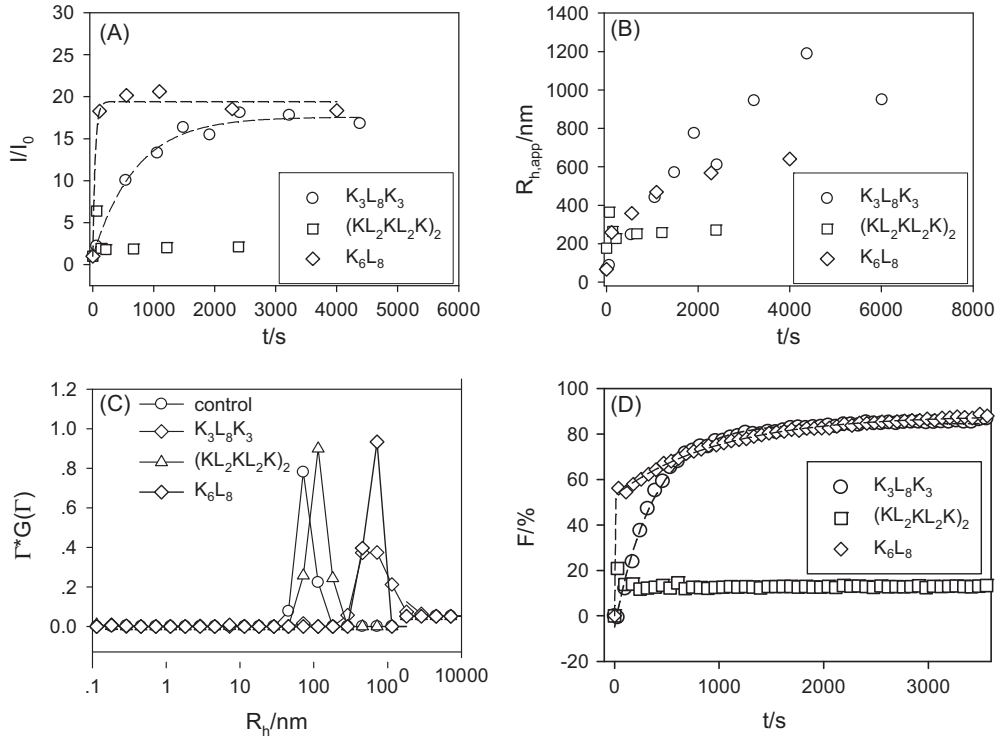

Fig. 5. The excess scattered intensity (A), $R_{h,app}$ (B), size distribution (C) and membrane fusion (D) of DPPC/DPPG LUVs after addition of $K_3L_8K_3$, K_6L_8, and (KL_2KL_2K). The peptide concentration is 25 μM; c(DPPC/DPPG) = 15.6 μM; $\rho_{p/l} = 0.053$. The dashed curves in Panels A and D are the fitting of the data.

most efficient approach to cause leakage. The "Barrel-stave", "carpet", and "toroidal-pore" are the most common models used to describe the membrane disruption mechanism [31]. In all these models, the leakage was more efficient if the peptides were able to insert inside the membrane instead of working in between membranes to cause aggregation or fusion [32,33]. Therefore, the aggregation and the fusion, which did not necessarily generate leakage, alleviated the antimicrobial activity by diversifying the functions of AMPs. $(KL_2KL_2K)_2$ in Table 2 met this criterion. An overshoot in aggregation was thus observed when the interaction location shifts from inter-particle (aggregation) to intra-particle (leakage) (Fig. 5A). The behaviors of K_6L_8 and $K_3L_8K_3$ also proved this viewpoint. Their chemical composition and chain length are the same as those of $(KL_2KL_2K)_2$, but their antimicrobial activities were much lower. This is likely due to their capability to induce efficient membrane aggregation or fusion. Another example was $(KL_2KL_3)_2$. Both $(KL_2KL_3)_2$ and $(KL_2KL_2K)_2$ formed amphiphilic α-helix structure. The only difference was that the former had a larger hydrophobicity/charge ratio. However, the antimicrobial efficiency of $(KL_2KL_3)_2$ was significantly reduced. This can be attributed to the non-specificity of $(KL_2KL_3)_2$ in causing membrane leakage, since relatively strong aggregation and fusion were also observed in the presence of $(KL_2KL_3)_2$ at the same conditions.

Table 2 also shows that $(KL_2KL_3)_2$ exhibited much strong activity in killing normal cells, in agreement with that higher hydrophobicity decreases cell-selectivity [3–5]. Unlike bacteria membrane, cell membrane contains negligible amount of negative charges [31]. The hydrophobic interaction was thus more important than electrostatic interaction when peptide interacts with cell membrane. Assuming leucines formed regular α-helix, the hydrophobic length of 8 connecting leucines was about 1.2 nm (0.15 nm × 8) [34], which was smaller than half of the thickness of cell membrane (the thickness of lipid bilayer is ~3.0 nm). Therefore, the cells were safe for that most of the 14-mer peptides shown in Table 2 cannot penetrate and disrupt the cell membrane. $(KL_2KL_3)_2$ was an exception. It formed an α-helix of 2.1 nm (more than half of the membrane thickness) and highly hydrophobic, significantly enhanced its power in destroying cell membranes. Although $(KL_2KL_2K)_2$ had the same length as $(KL_2KL_3)_2$, its lower hydrophobicity might compromise its ability in disrupting cell membrane. Therefore, both the hydrophobicity/charge ratio and the depth of the peptide inside the membrane were involved in the selectivity. The hydrophobicity/charge ratio should have an optimal value or value range, while the interaction depth, as indicated in our work, was related to the hydrophobicity of the peptide, and was likely in between half to 2/3 of the cell membrane.

It was not clear why $K_3I_8K_3$ and $K_6L_{16}K_6$ mediated no antimicrobial activities. $K_6L_{16}K_6$ had a strong tendency to self-aggregate in aqueous solution, leading to a heavy precipitation when contacting with liposome. As for $K_3I_8K_3$, the α-helix content (Table 1) was much lower than that of $K_3L_8K_3$. Other undefined reasons might explain the compromised membrane disruption activity of isoleucine.

5. Conclusion

In this study, a series of candidate AMPs composing of two amino acids (lysine and leucine in most cases) were designed and tested, in terms of antimicrobial activity, membrane aggregation, fusion, and leakage. No evident correlation was identified between the antimicrobial activity and the property of the peptides such as the sequence, length, hydrophobicity/charge ratio and secondary structure. However, common activities against model membrane were nevertheless found correlated with the antimicrobial activity, in that mediating efficient membrane leakage, negligible membrane fusion and liposome aggregation. These results indicated that when a peptide could mediate an efficient intramembrane interaction, it also leads to higher inhibition on bacteria growth.

Acknowledgement

This work was supported by the National Natural Science Foundation of China (21074005, 21174007).

Appendix A. Supplementary data

Supplementary data to this article can be found online at http://dx.doi.org/10.1016/j.bbamem.2014.08.018.

References

[1] (a) M. Zasloff, Antimicrobial peptides of multicellular organisms, Nature 415 (6870) (2002) 389–395;
(b) A.A. Strömstedt, L. Ringstad, A. Schmidtchen, M. Malmsten, Interaction between amphiphilic peptides and phospholipid membranes, Curr. Opin. Colloid Interface Sci. 15 (6) (2010) 467–478.
[2] (a) C. Subbalakshmi, N. Sitaram, Mechanism of antimicrobial action of indolicidin, FEMS Microbiol. Lett. 160 (1) (1998) 91–96;
(b) A. Patrzykat, C.L. Friedrich, L. Zhang, V. Mendoza, R.E.W. Hancock, Sublethal concentrations of pleurocidin-derived antimicrobial peptides inhibit macromolecular synthesis in *Escherichia coli*, Antimicrob. Agents Chemother. 46 (3) (2002) 605–614;
(c) K.A. Brogden, Antimicrobial peptides: pore formers or metabolic inhibitors in bacteria? Nat. Rev. Microbiol. 3 (3) (2005) 238–250.
[3] T. Wieprecht, M. Dathe, M. Beyermann, E. Krause, W.L. Maloy, D.L. MacDonald, M. Bienert, Peptide hydrophobicity controls the activity and selectivity of magainin 2 amide in interaction with membranes, Biochemistry 36 (20) (1997) 6124–6132.
[4] Z.Q. Jiang, B.J. Kullberg, H. van der Lee, A.I. Vasil, J.D. Hale, C.T. Mant, R.E.W. Hancock, M.L. Vasil, M.G. Netea, R.S. Hodges, Effects of hydrophobicity on the antifungal activity of α-helical antimicrobial peptides, Chem. Biol. Drug Des. 72 (6) (2008) 483–495.
[5] L. Ringstad, E. Andersson Nordahl, A. Schmidtchen, M. Malmsten, Composition effect on peptide interaction with lipids and bacteria: variants of C3a peptide CNY21, Biophys. J. 92 (1) (2007) 87–98.
[6] M. Dathe, M. Schümann, T. Wieprecht, A. Winkler, M. Beyermann, E. Krause, K. Matsuzaki, O. Murase, M. Bienert, Peptide helicity and membrane surface charge modulate the balance of electrostatic and hydrophobic interactions with lipid bilayers and biological membranes, Biochemistry 35 (38) (1996) 12612–12622.
[7] A.J. Beevers, A.M. Dixon, Helical membrane peptides to modulate cell function, Chem. Soc. Rev. 39 (6) (2010) 2146–2157.
[8] M.E. Houston, L.H. Kondejewski, D.N. Karunaratne, M. Gough, S. Fidai, R.S. Hodges, R. E.W. Hancock, Influence of preformed α-helix and α-helix induction on the activity of cationic antimicrobial peptides, J. Pept. Res. 52 (2) (1998) 81–88.
[9] L. Ringstad, A. Schmidtchen, M. Malmsten, Effects of single amino acid substitutions on peptide interaction with lipid membranes and bacteria-variants of GKE21, an internal sequence from human LL-37, Colloids Surf. A Physicochem. Eng. Asp. 354 (1–3) (2010) 65–71.
[10] L. Ringstad, L. Kacprzyk, A. Schmidtchen, M. Malmsten, Effects of topology, length, and charge on the activity of a kininogen-derived peptide on lipid membranes and bacteria, Biochim. Biophys. Acta Biomembr. 1768 (3) (2007) 715–727.
[11] (a) B. Deslouches, S.M. Phadke, V. Lazarevic, M. Cascio, K. Islam, R.C. Montelaro, T.A. Mietzner, De novo generation of cationic antimicrobial peptides: influence of length and tryptophan substitution on antimicrobial activity, Antimicrob. Agents Chemother. 49 (1) (2005) 316–322;
(b) U.H.N. Dürr, U.S. Sudheendra, A. Ramamoorthy, LL-37, the only human member of the cathelicidin family of antimicrobial peptides, Biochim. Biophys. Acta Biomembr. 1758 (9) (2006) 1408–1425.
[12] E. Nordahl, V. Rydengård, P. Nyberg, D. Nitsche, M. Mörgelin, M. Malmsten, et al., Activation of the complement system generates antibacterial peptides, Proc. Natl. Acad. Sci. U. S. A. 101 (2004) 16879–16884.
[13] L. Kacprzyk, V. Rydengård, M. Mörgelin, M. Davoudi, M. Pasupuleti, M. Malmsten, et al., Antimicrobial activity of histidine-rich peptides is dependent on acidic conditions, Biochim. Biophys. Acta 1768 (2007) 2667–2680.
[14] A.A. Strömstedt, M. Pasupuleti, A. Schmidtchen, M. Malmsten, Evaluation of strategies for improving proteolytic resistance of antimicrobial peptides by using variants of EFK17, an internal segment of LL-37, Antimicrob. Agents Chemother. 53 (2009) 593–602.
[15] L. Ringstad, A. Schmidtchen, M. Malmsten, Effect of peptide length on the interaction between consensus peptides and DOPC/DOPA bilayers, Langmuir 22 (2006) 5042–5050.
[16] L. Ringstad, E. Protopapa, B. Lindholm-Sethson, A. Schmidtchen, A. Nelson, M. Malmsten, An electrochemical study into the interaction between complement-derived peptides and DOPC mono- and bilayers, Langmuir 24 (1) (2007) 208–216.
[17] (a) P.F. Almeida, A. Pokorny, Mechanisms of antimicrobial, cytolytic, and cell-penetrating peptides: from kinetics to thermodynamics, Biochemistry 48 (34) (2009) 8083–8093;
(b) Sterling A. Wheaten, A. Lakshmanan, Paulo F. Almeida, Statistical analysis of peptide-induced graded and all-or-none fluxes in giant vesicles, Biophys. J. 105 (2) (2013) 432–443.
[18] (a) D.P. Siegel, W.J. Green, Y. Talmon, The mechanism of lamellar-to-inverted hexagonal phase-transitions-a study using temperature-jump cryoelectron microscopy, Biophys. J. 66 (2) (1994) 402–414;

(b) J. Bentz, H. Ellens, M.Z. Lai, F.C. Szoka, On the correlation between H_{II}phase and the contact-induced destabilization of phosphatidylethanolamine-containing membranes, PNAS 82 (17) (1985) 5742–5745;
(c) T.M. Allen, K. Hong, D. Papahadjopoulos, Membrane contact, fusion, and hexagonal (H_{II}) transitions in phosphatidylethanolamine liposomes, Biochemistry 29 (1990) 2976–2985;
(d) H. Ellens, J. Bentz, F.C. Szoka, Destabilization of phosphatidylethanolamine liposomes at the hexagonal phase transition temperature, Biochemistry 25 (1986) 285–294;
(e) H. Ellens, J. Bentz, F.C. Szoka, Fusion of phosphatidylethanolamine-containing liposomes and mechanism of the La–Hii phase transition, Biochemistry 25 (1986) 4147–4157.
[19] A.D. Bangham, R.W. Horne, Negative staining of phospholipids and their structural modification by surface-active agents as observed in the electron microscope, J. Mol. Biol. 8 (1964) 660.
[20] G.R. Bartlett, Phosphorus assay in column chromatography, J. Biol. Chem. 234 (1959) 466.
[21] (a) J. Wilschut, D. Papahadjopoulos, Studies on the mechanism of membrane fusion: kinetics of calcium ion induced fusion of phosphatidylserine vesicles followed by a new assay for mixing of aqueous vesicle contents, Nature 281 (1979) 690–692;
(b) J. Wilschut, N. Duzgunes, R. Fraley, D. Papahadjopoulos, Studies on the mechanism of membrane fusion: kinetics of calcium ion induced fusion of phosphatidylserine vesicles followed by a new assay for mixing of aqueous vesicle contents, Biochemistry 19 (1980) 6011–6021.
[22] S.W. Provencher, Contin — a general-purpose constrained regularization program for inverting noisy linear algebraic and integral-equations, Comput. Phys. Commun. 27 (3) (1982) 229–242.
[23] D.K. Struck, D. Hoekstra, R.E. Pagano, Use of resonance energy transfer to monitor membrane fusion, Biochemistry 20 (1981) 4093.
[24] Reference Method for Broth Dilution Antifungal Susceptibility Testing of Filamentous Fungi: Approved Standard, 2nd ed. Clinical and Laboratory Standards Institute, Wayne, PA, 2008. (M38-A2).
[25] J. Rizo, F.J. Blanco, B. Kobe, M.D. Bruch, L.M. Gierasch, Conformational behavior of *Escherichia coli* OmpA signal peptides in membrane mimetic environments, Biochemistry 32 (18) (1993) 4881–4894.
[26] http://lamar.colostate.edu/~sreeram/CDPro/main.html.
[27] K.A. Hammer, C.F. Carson, T.V. Riley, Susceptibility of transient and commensal skin flora to the essential oil of *Melaleuca alternifolia* (tea tree oil), Am. J. Infect. Control 24 (1996) 186–189.
[28] (a) M.B. Ruiz-Argüello, G. Basáñez, F.M. Goñi, A. Alonso, Different effects of enzyme-generated ceramides and diacylglycerols in phospholipid membrane fusion and leakage, J. Biol. Chem. 271 (43) (1996) 26616–26621;
(b) G. Basáñez, M.B. Ruiz-Argüello, A. Alonso, F.M. Goñi, G. Karlsson, K. Edwards, Morphological changes induced by phospholipase C and by sphingomyelinase on large unilamellar vesicles: a cryo-transmission electron microscopy study of liposome fusion, Biophys. J. 72 (6) (1997) 2630–2637;
(c) H. Zhao, R. Sood, A. Jutila, S. Bose, G. Fimland, J. Nissen-Meyer, P.K.J. Kinnunen, Interaction of the antimicrobial peptide pheromone Plantaricin A with model membranes: implications for a novel mechanism of action, Biochim. Biophys. Acta Biomembr. 1758 (9) (2006) 1461–1474;
(d) L.R. Montes, F.M. Goñi, N.C. Johnston, H. Goldfine, A. Alonso, Membrane fusion induced by the catalytic activity of a phospholipase c/sphingomyelinase from *Listeria monocytogenes*, Biochemistry 43 (12) (2004) 3688–3695.
[29] F.Y. Ke, Y.K. Luu, M. Hadjiargyrou, D.H. Liang, Characterizing DNA condensation and conformational changes in organic solvents, PLoS ONE 5 (10) (2010).
[30] A. Giacometti, O. Cirioni, W. Kamysz, G. D'Amato, C. Silvestri, M. Simona Del Prete, J. Lukasiak, G. Scalise, In vitro activity and killing effect of the synthetic hybrid cecropin A–melittin peptide CA(1–7)M(2–9)NH2 on methicillin-resistant nosocomial isolates of Staphylococcus aureus and interactions with clinically used antibiotics, Diagn. Microbiol. Infect. Dis. 49 (3) (2004) 197–200.
[31] K.A. Brogden, Antimicrobial peptides: pore formers or metabolic inhibitors in bacteria? Nat. Rev. Microbiol. 3 (3) (2005) 238–250.
[32] K. Matsuzaki, O. Murase, N. Fujii, K. Miyajima, An antimicrobial peptide, magainin 2, induced rapid flip-flop of phospholipids coupled with pore formation and peptide translocation, Biochemistry 35 (1996) 11361–11368.
[33] L. Yang, T.A. Harroun, T.M. Weiss, L. Ding, H.W. Huang, Barrel-stave model or toroidal model? A case study on melittin pores, Biophys. J. 81 (2001) 1475–1485.
[34] R.H. Garrett, C.M. Grisham, Biochemistry, 2nd ed. Saunders College Publishing, USA, 1999.